A Fully Programmable White-Rabbit Node for the SKA Telescope PPS Distribution System

Miguel Jiménez-López, Felipe Torres-González, Jose Luis Gutiérrez-Rivas, Manuel Rodríguez-Álvarez, and Javier Díaz

***Abstract*— Distributed data acquisition (DAQ) systems are in charge of converting different analog environment signals into digital values to perform control and monitor tasks. They require a computer network technology to share data between their different elements. One of their main issues is to match data with the specific events under study. A possible solution is to include an event synchronization technology such as Network Time Protocol (NTP), Precise Time Protocol (PTP), or White Rabbit (WR). This contribution proposes a high-performance distributed timing system based on the WR technology. We focus on the square kilometer array (SKA) project as an example of the distributed DAQ system. The SKA project has a strict timing requirements for its operation with a performance below 2 ns. This accuracy is not achievable by current standard synchronization technologies such as NTP or PTP. Under this context, the authors propose the WR zynq embedded node (WR-ZEN) platform as a candidate for the SKA's pulse per second (PPS) distribution system. It is a new design that integrates the WR technology, thus enabling the subnanosecond accuracy. Finally, the WR-ZEN has been evaluated in different scenarios to demonstrate its timing performance in dynamic environment conditions fulfilling the SKA telescope requirements for PPS distribution.**

***Index Terms*— Gigabit Ethernet, network, optical fiber, square kilometer array (SKA), synchronization, White Rabbit (WR).**

I. Introduction

AT PRESENT, there are many industrial [1] and scientific applications [2] that require data acquisition (DAQ) systems [3]. Their main purpose is the study of physical phenomena converting the analog environment signals into digital values. DAQ systems include a specific node that is responsible for receiving, processing, and extracting critical information related to a certain event. Because of the distributed nature of DAQ systems, it becomes mandatory to define some mechanisms to match event data acquired in different nodes. One possible solution is to deploy a synchronization technology in the distributed DAQ network sharing the time information between different nodes and then, the events can be identified by the time they occurred.

Manuscript received April 4, 2018, revised May 27, 2018, accepted June 5, 2018. Date of publication July 18, 2018; date of current version December 24, 2018. This work was supported in part by the Horizon 2020 ASTERICS under Grant 653477 and in part by VITVIR, Junta de Andalucia under Grant TIC-8120 and Grant 614 AYA2015-65973-C3-2-R AMIGA6. The Associate Editor coordinating the review process was Mojtaba Hosseini. *(Corresponding author: Miguel Jiménez-López.)*

The authors are with CITIC, ETSIIT, University of Granada, 18010 Granada, Spain (e-mail: klyone@ugr.es).

Color versions of one or more of the figures in this paper are available online at http://ieeexplore.ieee.org.

Digital Object Identifier 10.1109/TIM.2018.2851658

There are many mechanisms to spread time information and signals in distributed systems. Some of them use global navigation satellite system receivers to get timing from satellites [Global Positioning System (GPS), Global'naya Navigatsionnaya Sputnikovaya Sistema [4], Galileo [5]) meanwhile others use wired protocols [National Marine Electronics Association Protocol, Interrange Instrumentation group time code (IRIG-B)] to disseminate the time reference through the network. The GPS approach is widely used in systems that require accurate synchronization since devices can be easily connected to different GPS receivers as stated in [6]. The main concern related to GPS systems regards to their exposure to jamming and spoofing attacks. Alternatively and thanks to the popularity of Ethernet packet networks, timing protocols are being imposed gradually as the main time transfer solution. Low-performance protocols such as Network Time Protocol (NTP) [7] are widely used in standard applications while the industrial domain requires a more precise protocol like the IEEE-1588v2 also known as Precise Time Protocol version 2 (PTPv2) [8], [9]. PTPv2 is an industrial evolution of NTP, characterized by the utilization of hardware (HW) timestamp mechanisms that significantly improves the time synchronization accuracy. Typically, NTP provides about 1-ms synchronization accuracy, while PTPv2 is able to achieve an accuracy about 50 ns. PTPv2 is a candidate technology for control applications such as smart grid where the time requirements are very strict and the synchronization is one of their key aspects [10]. The smart grid applications also need switchover mechanisms that can be improved using high accuracy synchronization [11] and require calibration procedures [12] to match the event information present in the network properly. Note that the previous technologies only solve partially the synchronization problem by means of provision of a time reference such as coordinated universal time (UTC) or international atomic time encoding a pulse per second (PPS) signal. However, they do not provide frequency dissemination as is required in the analog-to-digital converter (ADC)/DAQ components of the distributed DAQ systems.

Some scientific facilities need a specific distributed DAQ system due to their strict timing requirements that cannot be achieved by commercial solutions. One example is the square kilometer array (SKA) [13] international project whose goal is to build a radio telescope tens of times more sensitive and hundreds of times faster at mapping the sky than today's best radio astronomy facilities. The SKA telescope is composed of

several types of antennas settled over long distances forming a distributed DAQ system, hence requiring data sharing and synchronization networks. Different technologies and solutions were analyzed for the SKA timing system such as GPS or standard packet-based protocols (NTP, PTP, and PTPv2). However, these solutions are not appropriated to fulfill the SKA's strict timing specifications (2 ns for the SKA telescope). Under this context, the authors of this paper are currently working as a partner in the SKA signal and data transport (SaDT) [14] work package. Our proposal consists in the development of a new device based on the technology called White Rabbit (WR) [15] to disseminate a PPS signal very accurately over fiber links. WR is an evolution of the PTPv2 protocol, being able to distribute an absolute time reference with an accuracy below 1 ns. The equipment located at each endpoint delivers a PPS signal with its edge aligned to the start of the UTC second. Therefore, each telescope can then be phased up by observing the white light fringe on one or more bright, compact sources.

This contribution describes a new high accuracy platform to fulfill SKA telescope requirements and it is organized on several sections. The current one presents the introduction and the motivation. Section II introduces the SKA telescope project and its timing requirements which evidence that current industrial solutions are not suitable for SKA. Section III focuses on the fundamentals of the WR technology. Section IV describes the proposed endnode for SKA including the justification, architecture, and software support. Section V includes different scenarios to evaluate the scalability of the WR technology and the synchronization accuracy taking into account different meteorological conditions. Final remarks and conclusion are described in Section VI.

II. SKA Telescope

SKA will be the world's largest radio telescope and it will be located in two different geographical areas: South Africa and Australia/New Zealand. There are two locations for the SKA facility in order to cover several frequency ranges for the sky observations [16]. It will be constructed in different phases: SKA1 (phase 1; 2018–2023) and SKA2 (phase 2; 2023–2033). The development will be deployed using two different pathfinders existing on each place (MeerKAT in South Africa [17] and ASKAP in Australia [18]). SKA1 starts in 2018 and it is intended to cover the 10% of the total area at low and mid frequencies by 2023. SKA2 has the goal to get the full array working at low and mid frequencies by 2030.

The SKA telescope uses different types of networks to guarantee a proper operation of the infrastructure. The design of the network corresponds to the SaDT element [14], and it includes all the necessary HW and software for the transmission of data and information between the elements of SKA. SaDT also contains details about the provision of timing which is critical for interferometry. The final part of the SaDT is the synchronization and timing (SAT) that provides frequency and clock signals from a central clock ensemble to all elements of the system to maintain the same phase information on all receptors, timing signals for data identification, and time-critical activities. In order to maintain phase coherence across the array, it requires a short-term timing precision of around 1 ps, while an accuracy of 10 ns for 10-year periods becomes mandatory for long-term timing pulsar requirements. This contribution focuses on the high accuracy synchronization method used for SKA responsible to provide a PPS signal to the critical elements.

A. High Accuracy Timing Signals Distribution for SKA1

As determined by SaDT, the SKA telescope should be able to distribute a common frequency reference to all the antennas in order to provide a unique time reference to register all the events with ultrahigh accuracy using timestamps. This task is performed by the SAT element that belongs to SaDT. It is important to remark that SaDT uses different mechanisms to achieve frequency dissemination and PPS distribution goals, but our contribution only addresses a suitable candidate solution for the second issue. Boven [19] summarizes the PPS distribution requirements. As previously presented, it is constrained to 10 ns. However, the UTC realization error must be bounded below 5 ns, and the synchronization technology for the SAT network has only a 2-ns quota for the PPS distribution. This system will be in charge of delivering its output at the following locations: SKA1-MID with 133 dishes connected to optical fiber links between 120 and 150 km and SKA1-LOW with 45 stations along three spiral arms connected to optical fiber links between 70 and 80 km. Depending on the frequency offset scheme applied to all SKA1-MID dishes, additional 64 endpoints may be needed in SKA1-MID. By this, the synchronization network might be increased from 182 to 246 endpoints. In addition, SKA1 uses aerial optical fiber networks that are significantly affected by the large temperature excursion during operation, presenting variations of more than 20 °C in desert locations, such as South Africa and Australia. Furthermore, outdoor wind velocities during normal operation could achieve up to 40 km/h, making fibers oscillate, changing their length, and forcing to develop a compensation mechanism on real-time during execution.

An additional issue for the SKA synchronization network is the Sagnac effect [20]. Normally, it is negligible for short fiber links; however, it is not the case for SKA infrastructure where the Sagnac effect has been calculated for a 80-km East–West SKA link obtaining a deviation of 350 ps as described in [21].

As a summary, the SKA telescope has a quite challenging goal because it imposes a high accuracy synchronization requirement and also for the dynamic environmental operation conditions of the facility. Section III describes the WR technology introducing its main features and its different network elements.

III. White Rabbit Synchronization Protocol

The WR technology [22] is an open source and international collaborative project started at CERN in 2009, later joined by other worldwide laboratories and companies. WR was launched as an open short wave /HW initiative with available online sources at CERN's open HW repository [23]. Thanks to its versatility and improved performance compared

to other alternatives, it was quickly adopted by other scientific institutions and some private companies such as seven solutions or Creotech which are interested in extending WR for industrial solutions. Some examples of that effort are the projects WR-SYNTEF [24] and IFMIF/EVEDA [25].

The WR protocol extends PTPv2 with extra messages and has been proposed to be included in the new PTP release as high accuracy profile [26]. Its main goal is to provide synchronization accuracy better than 1 ns and precision in the scale of picoseconds addressing weak aspects of the PTPv2: the limitation of the phase difference measurements to one period of the system clock; and the assumption of symmetry between transmission and reception paths. The first issue is solved implementing a frequency synchronization alongside a fine phase measurement procedure. The former consists of recovering the clock from the physical layer (L1) and using it to adjust the local oscillator using a proportional-integrator servo algorithm. The latter employs a dual mixed time difference method that is able to overcome the one-cycle time resolution limitation, and it can be implemented in digital designs [27] allowing to achieve subpicosecond resolution. To solve the second issue, WR add new parameters to the PTP implementation to consider the link asymmetry, small form-factor pluggable (SFP), and gateware delays. For bidirectional fibers, see the calibration method of [28] which estimate the asymmetry factor due to the speed difference associated with using different wavelengths for the transmission and reception channels of the optical link.

Other contributions propose alternative ways to perform the frequency synchronization and estimate the synchronization uncertainty. The former can be faced using oversampling method [29]. It requires a high rate exchange of timing packets reducing the available bandwidth for the applications and its timing performance can be affected in extreme conditions such as network congestion. The latter [30] proposes a different clock servo loop based on the Kalman filter which is able to calculate the synchronization uncertainty improving the timestamp accuracy.

WR implements mechanisms to ensure deterministic and reliable data transfer between thousands of nodes connected over optical fiber links up to 10 km. However, it can easily be extended up to 50 km without significant degradation and up to 120 km without the need of optical amplification. One application of the WR for long links can be found in [31].

A. Network Topology

A typical WR network presents a tree topology and is composed of three different kinds of elements: a grandmaster (GM), several intermediate devices such as switches, and endnodes as shown in Fig. 1. The GM is normally connected to a very stable clock such as an atomic clock or a GPS receiver [32]. The intermediate levels of the network disseminate the timing packets to the final nodes using the master–slave scheme. These devices have several ports and can behave as PTPv2 boundary clocks (BCs). The nodes of the last level of the network are known as slave devices. They recover the clock reference from the link and synchronize their local oscillators in order to provide a time reference for a specific application.

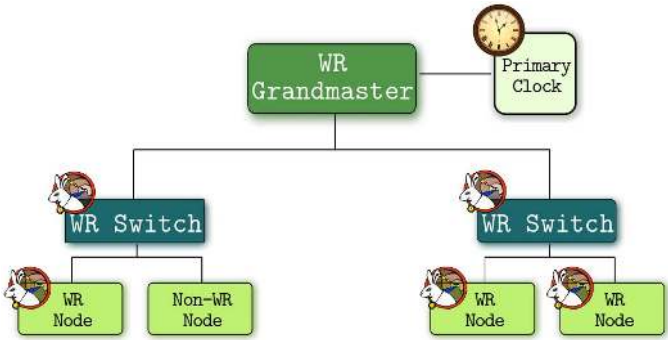

Fig. 1. WR network is a tree hierarchy where the root node is the GM that distributes the reference time signals. The intermediate elements are WRS that acts as BC propagating the time signals from the upper layers of the network. Finally, the main purpose of the endnodes is to provide timing to another specific application.

In addition to the conventional tree topology of the timing networks, new network topologies are currently under study in WR to add some mechanisms to improve fault tolerance and security. Examples of this paper are in [33] and [34] which incorporate transparent clocks and redundancy protocols into the WR technology such as high-availability seamless redundancy to ensure data delivery and reception in critical applications such as control network, real-time applications, or smart grids.

B. WR Devices Survey for the SKA Telescope

Regardless of the case of use for the WR technology, it will be needed to select a suitable set of WR devices. Most applications distinguish between two main roles according to a typical WR network: devices that act as BC, and those that act as ordinary clocks (OCs). Currently, the WR switch (WRS) [35] is the most convenient BC among all the WR devices because of its 18 SFP slots. However, there are several WR platforms that can act as OCs. Therefore, we have analyzed three devices taking into account the specific requirements of the SKA project: the simple peripheral component interconnect express (PCIe) field-programmable gate array (FPGA) Mezzannine Card (FMC) carrier simple PCIe FMC carrier (SPEC) [36], the WR light-embedded node (WR-LEN) [37], and the WR zynq-embedded node (WR-ZEN) [37]. The former could be used in a standalone mode [38] but due to its limited computational resources, the usually SPEC used is connected to a host PC using the PCIe interface. The WR-LEN is a standalone WR node with good timing performance, but it does not provide advanced software capabilities. The latter presents several improvements compared to the rest of WR nodes such as a novel architecture based on a Xilinx FPGA-SoC together with a dual-core ARM microprocessor [39] and an improved low-noise clocking circuitry. Because of the previous discussed advantages, the WR-ZEN has been chosen as the candidate platform to implement the PPS distribution system for SKA.

Section IV provides the description of the authors' proposed solution for the SKA telescope PPS distribution system.

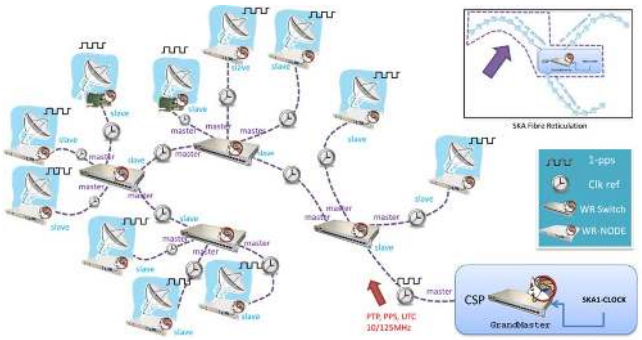

Fig. 2. Network topology for PPS signal distribution based on WRSs and nodes.

IV. PPS Distribution System for SKA

The WR protocol requires a network topology similar to the International Telecommunication Union-T G.8275. 1-/Y.1369.1 standard, a PTPv2 telecommunication profile that describes a time-aware network capable to provide full timing support [9] as explained in Section III. It uses a master time reference (SKA1 clock) that is distributed following a tree topology in a master–slave configuration as is shown in Fig. 2. The SKA PPS distribution system is composed of two different kinds of devices.

1) The WRSs [37] are placed in the CSPs at each of the clock ensembles. For SKA1-MID, one is placed halfway along each of the three spiral arms to regenerate the signal for the longest links.
2) The endnodes (WR-ZEN [37]) will be located at the cores of SKA1-LOW and SKA1-SURVEY, along their spiral arms, one for each SKA1-MID dish and one for each CSP.

The synchronization between WR devices is performed over a single fiber link up to 120 km using commercial SFPs. However, the distances for SKA1-MID are longer and it is necessary to use intermediate WRSs as repeaters with a penalty over the system performance due to the increment of the inherent noise of each WR device. This noise is propagated to the downstream nodes. An analysis of the jitter evolution depending on the number of hops can be read in [40]. Thanks to the network similarities between WR and SKA, the same single fiber strand can be used for the SAT network.

An important feature of the system is that the PPS at each station is derived from the reference frequency distributed from the SKA clock and not from the WR system. In normal operation, the WR system only monitors the absolute time of each PPS and reports it back activating an alert if the PPS signal is not aligned to the start of the UTC second. This condition indicates a malfunctioning in the timing chain so that the station must discard data to avoid system data corruption. Other functionality associated with the WR part is to temporarily alter the division ratio to bring the PPS edge back in alignment with UTC time. In this case, fringe finding must then be performed to restore the full calibration again.

The centrally located WRSs and the WR endnodes are connected to a single strand of a single-mode fiber with LC/PC connectors and industry standard bidirectional SFPs that use two wavelengths (downstream and upstream) to produce optical signals to be transmitted. Finally, the endnodes generate a valid PPS signal.

A. PPS Distribution Node Architecture

The PPS distribution system for SKA is based on the WR-ZEN platform that provides the WR support that ensures the synchronization accuracy in the system. The first design of the PPS system includes the fine delay FMC card that is used to generate the timing signals through mezzanine channels. Moreover, it has two network interface cores (NICs) that allow accessing optical fiber ports as conventional Linux network interfaces. An introduction to this platform is presented in [41], and a contribution that improves the NIC bandwidth of the design in [42]. In addition, the WR-ZEN is also under study using other FMC cards such as the FMC ADC card to build a distributed oscilloscope [43].

At present, the utilization of the fine delay FMC card [44] is still under discussion, and there is a possible design that the final architecture could be addressed without this module.

1) HW and Gateware: The HW includes a Xilinx Zynq FPGA-SoC and an enhanced clocking scheme that improves the clock stability. As described in [45], the WR general performance is limited by noise when locking to an external reference, in the so-called GM mode. Therefore, in order to decrease the noise, internal phase-locked loops (PLLs) in the FPGA should be avoided and an external PLL is recommended.

The gateware (FPGA firmware) is shown in Fig. 3. Its components are connected through a wishbone crossbar that enables the processor configuration. It includes the White Rabbit PTP Core (WRPC)-2p [40] core that implements the high accuracy timing protocol based on WR and provides basic network and debug capabilities. The gigabit transceiver port (GTP) and NIC modules are in charge of processing the incoming/outgoing packets and notify these events to the processor. The transmission timestamp unit stores the outgoing packet timestamps. The fine delay core controls the operation of the fine delay FMC card if any is plugged into the FMC socket.

2) Firmware and Software: The firmware code performs all the WR functionalities and it runs in the soft microprocessor inside the WRPC-2p core. Its main tasks are: 1) the servo loop algorithm, which maintains the local oscillator locked to the recovered master's frequency and 2) the implementation of the WR-PTP stack.

The software components are presented in Fig. 4 and are divided into the user-space utilities and the kernel support. The former includes the *Zen library* and the *Zen tools* that enable the FPGA programming and access to internal devices such as an universal asynchronous receiver transmitter for debugging/configuration and among others. In the kernel side, some drivers have been implemented to control the entire platform.

Section V describes the main performed experiments and the obtained results using the WR-ZEN.

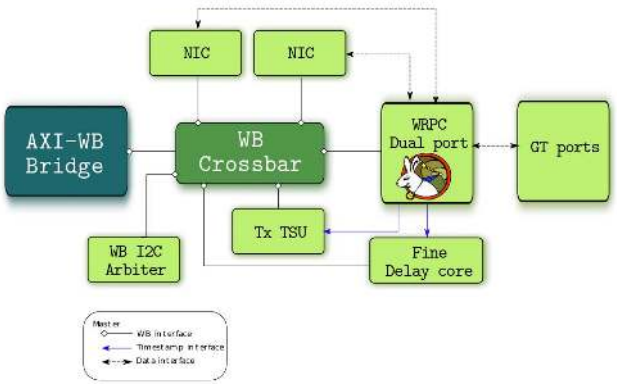

Fig. 3. WRPC-2p implements the WR protocol, the GT ports and NIC cores allow to receive/transmit Ethernet packets through the SFP interface and the fine delay core controls the FMC card.

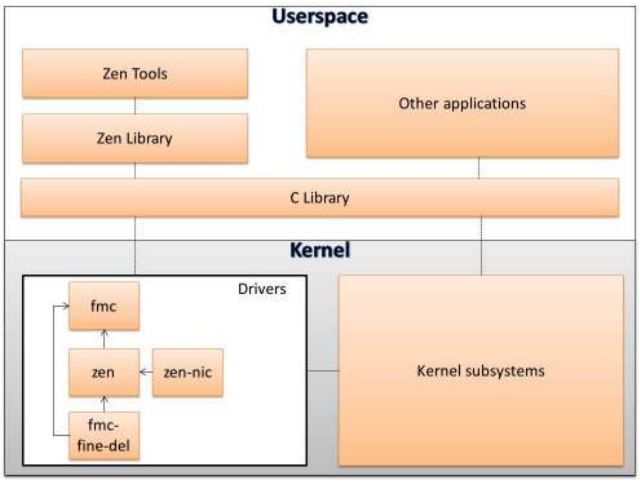

Fig. 4. WR-ZEN software is composed of different components such as the Linux kernel, some specific drivers and custom user-space applications.

V. Experiments and Results

In this section, we detail the experiments performed to demonstrate that the WR-ZEN is a suitable node for the SKA telescope PPS distribution system and the results obtained. In order to evaluate properly the project's timing requirements, we have performed three experiments: 1) a stability comparison between the three WR nodes analyzed in Section III-B; 2) a scalability test for the SKA network; and 3) a performance evaluation of the PPS stability under variable thermal conditions. The setup is depicted in Fig. 5, and the principal equipment and tools utilized during the experiments are: two WRSs to simulate two hops WR network (HW v3.4 and firmware v5.0), a WR-LEN (HW v1.0), a SPEC board with a digital input–output FMC, two WR-ZENs (HW v3.0 and firmware v1.2), and a Keysight high-resolution counter (52320A). Some additional components are necessary to establish the communication paths such as SFP modules (AXCEN 1310/1490 nm for short links and GE-BX-80 1490/1550 nm for larger scenarios), simplex optical fiber links (G652D): short fibers for device characterization and longer ones (20 and 50 km) for the scalability and temperature

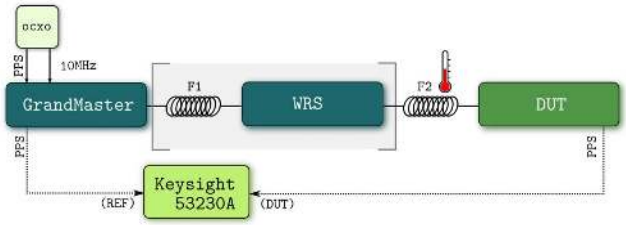

Fig. 5. Block diagram of the different experiment configurations for the PPS stability, network scalability, and temperature influence test using a climatic chamber.

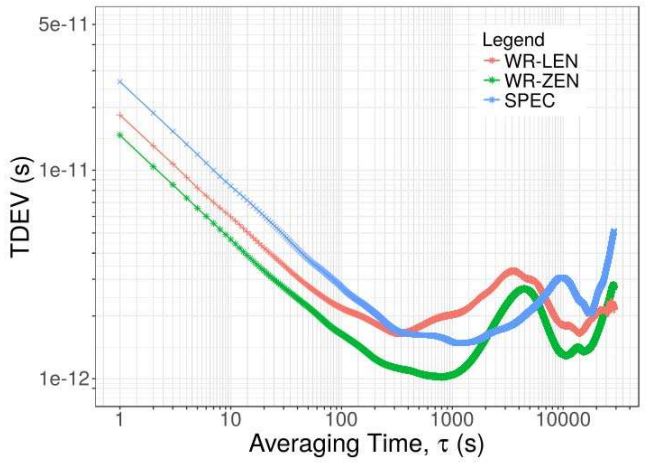

Fig. 6. TDEV plot for the three analyzed WR nodes as slaves of a WRS.

tests and an OCXO Morion MV89 as a frequency reference for the GM mode.

A. PPS Performance

The PPS performance is evaluated for the three WR nodes as previously described. The GM is a WRS, to which the three nodes are connected. Regarding Fig. 5, F1 and the second WRS are not included in this setup. F2 is a 0.5-m fiber link, under laboratory conditions. Each node is connected to the same WRS with a short fiber link. Once the node is fully synchronized, we start to measure the time interval between the PPS from WRS and PPS from the slave node. All measurements have been carried out for 24 h under laboratory conditions.

Fig. 6 corresponds to the time deviation (TDEV) statistic. It expresses the stability of the phase difference between the WR master and WR slave versus the observation interval, τ. For a $\tau = 1$ s, we obtained a TDEV value of 1.47e-11 s for the WR-ZEN. This is 3.6e-12 s and 1.18e-11 s less than WR-LEN and SPEC, respectively. The lowest value is 1.0e-12 s for the WR-ZEN. Differences between the lowest values of WR-LEN and the SPEC board respect to the WR-ZEN are: 6.2e-13 and 4.6e-13 s respectively.

Modified Allan deviation (MDEV) results are included in Fig. 7. From the TDEV (6) and MDEV (7) results, we observe that white phase modulation (PM) noise dominates from $\tau = 1$ s to a few hundred seconds averaging

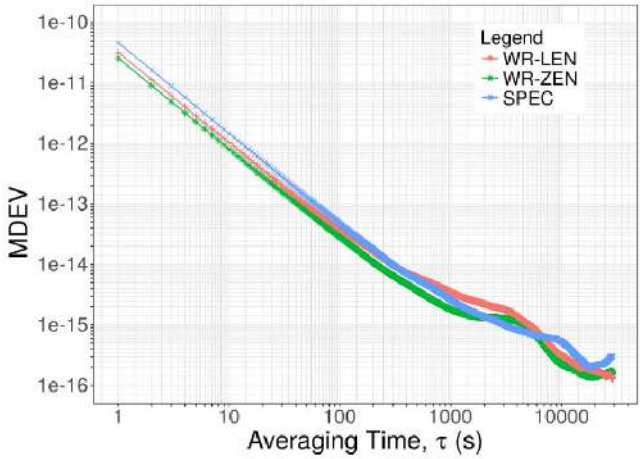

Fig. 7. MDEV plot for the three analyzed WR nodes as slaves of a WRS.

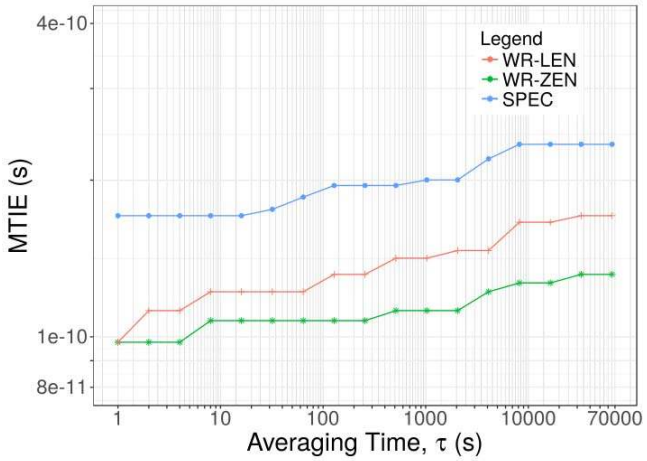

Fig. 8. MTIE plot analyzes the worst case scenario for the three WR nodes.

TABLE I
TDEV AND MTIE RESULTS FROM THE SCALABILITY TEST

	TDEV (s)	MTIE (s)
τ (s)		
1	2.32e-11	1.36e-10
8	6.51e-12	1.36e-10
64	2.37e-12	1.46e-10
512	4.38e-12	1.61e-10
1024	7.27e-12	1.66e-10
2048	9.75e-12	1.75e-10
4096	7.97e-12	1.90e-10

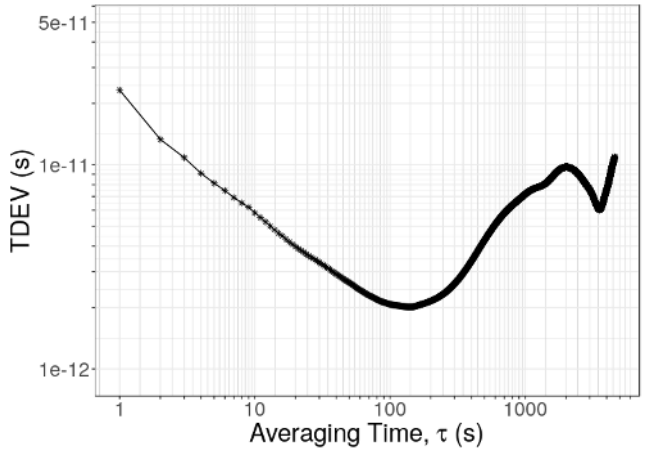

Fig. 9. TDEV plot comparing the PPS signal from the endnodes (WR-ZEN) to the GM of the network.

time (depending of the observed device). Afterward, the rest remains as flicker PM noise.

Finally, the worst case analysis has been performed with the maximum time interval error (MTIE) statistic (Fig. 8). With the MTIE results, we observed that all the WR devices fulfill the 2-ns time budget requirement even for the worst case scenario. For the WR-ZEN, the difference between the WRS PPS and its PPS is bounded on 1.5e-10 s. Again, the WR-ZEN achieves the best results: 3.90e-11 s less than the WR-LEN and 1.02e-10 s less than the SPEC.

The obtained values reveal that the proposed solution fulfills the requirements to be used in the SKA telescope's PPS distribution system. In Sections V-B and V-C, we evaluate the goodness of the solution in terms of scalability and taking into consideration the dynamic environment conditions.

B. WR Scalability for SKA

The next experiment covers a scalability analysis of the WR solution for the SKA timing system. In Section II, we presented an estimation of the final nodes that would be needed to be synchronized for the SKA: around 250 endpoints that must be synchronized with an accuracy below 2 ns.

We set up a test network as included in Fig. 5: a WRS as GM, a second WRS as intermediate BC, and an endnode such as the WR-ZEN. F1 and F2 are 20-km fiber spools under laboratory conditions. The selected SFPs are fiberstore ones (SFP-GE-BX80 with 1490-/1550-nm wavelengths). The PPS phase difference between the WR-ZEN and WRS in the GM mode has been measured using a Keysight 52320A counter for 4 h. This network configuration with only two hops is suitable to synchronize up to 306 endnodes using BC WRSs.

TDEV and MTIE values have been calculated by octaves, and the numerical values can be found in Table I. For the short-term stability, we obtained a TDEV result of 2.32e-11 s. The minimum is reached at $\tau = 64$ s, afterward, it is observed a frequency drift from $\tau = 200$ s to $\tau = 1000$ s (see Fig. 9). The MTIE results show that the maximum PPS error, during this test, is bounded below 2e-10 s (see Fig. 10).

With those findings, it has been proven that a WR network with two levels can provide synchronization to all the equipment expected for the SKA facilities. It is also important to mention that some links could be divided into two WR links due to the distance between some antennas (e.g., adding a WR

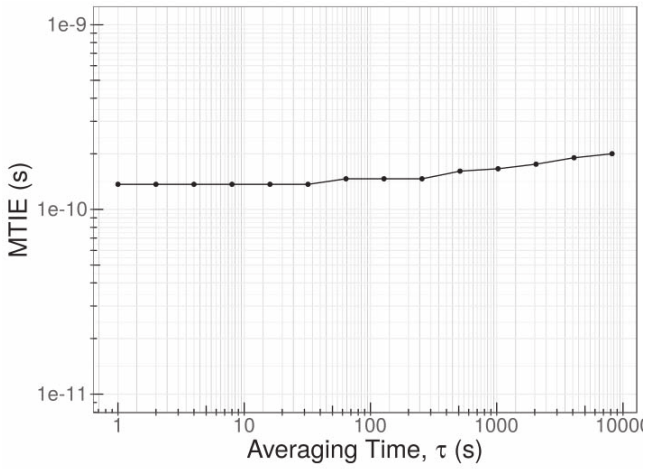

Fig. 10. MTIE plot for the scalability test. The endnode (WR-ZEN) is compared to the GM of the network.

device between the master WRS and the endnode). Introducing an extra WR level for some antennas should not be a problem to fulfill the timing requirements, a proof of that can be found in [40], where the results show that even a 10-hop network can reach the required time budget for SKA.

Although long-distance fiber links have been used for this test, thermal influence should be considered before confirming the goodness of the WR solution for the SKA's timing distribution system.

C. Temperature Influence on Time Accuracy

The WR network in the SKA deployment will be composed of long-distance aerial fiber links. Under variable climatic conditions, the propagation path of the light inside the fiber links may vary. Effects such as fiber bending, thermal expansions of materials, or changes in the refractive index would deteriorate WR's performance.

An accurate estimation of the one-way delay between two WR devices is mandatory to adjust properly the offset between devices, thus WR does not assumes a symmetric link. WR uses wavelength-division multiplexing to allow a duplex communication link. Despite the physical path is the same in both the directions, the optical path is not due to difference in the speed propagation associated with the wavelengths on each transmitter. This asymmetry is modeled on a asymmetry factor (α) and is assumed to be constant on the WR's link model [22], [32]. Conversely, the challenging environmental SKA conditions demand for further consideration regarding the temperature effect over chromatic dispersion and, therefore, dependencies of alpha with the temperature [46].

The proposed system has been tested by JIVE [47] in the SKA-specific dessert zones of the South Africa, and Boven [21] describes the main issues that must be taken into consideration. In this paper, we have focused on the temperature effect over the cable *round-trip* time (CRTT) and the PPS performance.

In order to evaluate that effect, we have introduced a 50-km fiber spool (F2) in a climate chamber. In this experiment, F1 and the WRS shown in Fig. 5 have not been used. Furthermore, the GM node was another WR-ZEN. The CRTT and the master–slave PPS offset have been measured for a temperature range from 20 °C to 50 °C with 10 °C steps. We expected to bound the accuracy degradation due to a temperature change in the propagation medium. All the measurements of the dependent values, such as CRTT and PPS offset, were accomplished right after reaching the target temperature. The WR equipment was calibrated to compensate the characteristic delays of each device following the official calibration procedure [28].

The most relevant results are included in Table II: 1) the mean value of CRTT and PPS offset samples and 2) their sample standard deviation. A total of 7200 samples (2 h) per temperature step have been used to compute the presented statistics. The amplitude of the CRTT sampled data is 96 496 ps. Dividing it by the temperature range, we obtained a CRTT variation of 3213 ps/°C. It is important to remark the huge variation in the propagation delay. Considering a synchronization system that is not capable of dynamically calibrating the change, the final performance would suffer from an enormous degradation, which is unacceptable for the SKA equipment. The peak-to-peak difference for the PPS

TABLE II
RESULTS OF THE THERMAL CHARACTERIZATION FOR AN OPERATIONAL FIBER TEMPERATURE IN RANGE 20 °C-50 °C WITH 10 °C STEPS

	RTT (ps)		**PPS** $offset_{SM}$ **(ps)**	
Spool temp (°C)	$\overline{x}$	s	$\overline{x}$	s
20	478471695	303	193	17
30	478503719	50	203	17
40	478533492	807	150	17
50	478567050	399	110	14

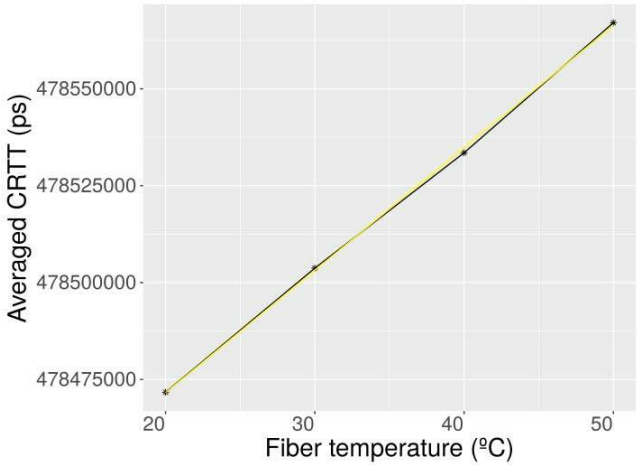

Fig. 11. Relationship between the fiber temperature and the cable round-trip time. Yellow line: perfect fit between both variables.

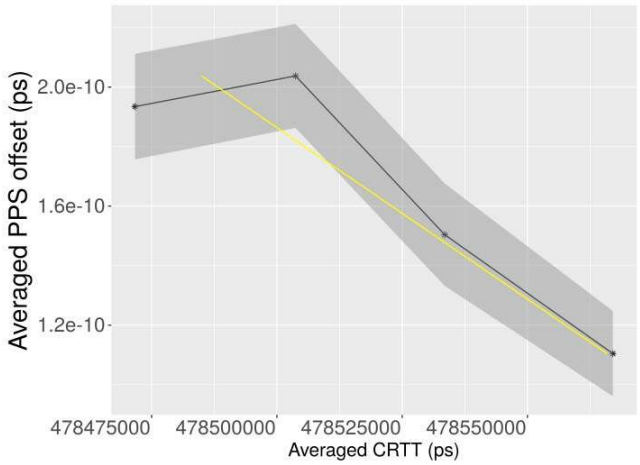

Fig. 12. Evaluation of the cable *round-trip* time and the PPS offset with variable temperature conditions for the fiber link. A linear fit model is included with the yellow line.

offset is 211 ps which leaves us a 7 ps/°C, and if we divide by the total link length: 0.14 ps/°C · km.

Fig. 11 shows a clear linear dependence between the temperature and the CRTT. A perfect fit between the variables is shown with a yellow line. If we compare the fit with the experimental data, we can affirm the high level of correlation between the fiber temperature and the CRTT, although the PPS offset is not constant as we suppose in our initial hypothesis. Fig. 12 suggests an inverse linear dependence between CRTT and the offset, expressed with a yellow line (linear fit). It must be considered that α is computed experimentally using a fixed-point arithmetic. While it seemed to work properly for distances shorter than few kilometers, it may be insufficient for such long distances as the ones used in our experiments. Nevertheless, the observed offset variation for a long distance link and a 30 °C temperature gradient is only 2e-10 s. This together with the results from the previous experiments makes the new PPS distribution system suitable for the SKA timing system.

VI. Conclusion

The contribution presented by the authors is based on a PPS distribution system using the WR technology as a candidate for the SKA telescope timing system. The strict timing requirements of this project requires the utilization of novel timing technologies able to provide an accuracy below 2 ns. This accuracy is not achievable using current standard timing protocols such as NTP and PTP. For this reason, authors proposed a solution based on the WR-ZEN that improves the existing WR node designs due to the inclusion of advanced software capabilities, a new gateware design compliant with high accuracy protocols, and an enhanced clock circuitry, being able to provide timing accuracy below 2 ns. Regarding advanced software capabilities, we have developed a Linux-based environment with some user-space tools and drivers. The gateware design implements the WR protocol and some additional FMC functionalities. The enhanced clocking circuitry can be configured using different schemes to offer the best synchronization performance and quality results targeting the SKA needs.

Several tests have been performed to evaluate the goodness of our proposal for the SKA PPS distribution system. Results demonstrate that the synchronization accuracy is bounded below 200 ps, being significantly better than the SKA needs. Moreover, the scalability tests reveal that the synchronization accuracy is maintained for hundreds of nodes with several network levels. Furthermore, additional experiments have been designed to simulate the SKA climatic place conditions to evaluate the thermal change influence in the propagation delay and its repercussion in the PPS distribution system. The obtained results evidences that the propagation delay increases tens of nanoseconds (96 ns) due to the temperature changes, but alongside that, the PPS offset maintains its accuracy with an offset not exceeding hundreds of picoseconds (211 ps). The experimental results demonstrate that the proposed solution outperforms the exigent SKA requirements taking into consideration the scalability needs of SKA and the harsh environmental condition of the telescope locations. Finally, it is important to remark that all these features are fulfilled using a standalone node that combines high-level applications integrated into a Linux OS including operational functionalities such as monitoring and control services mandatory to ensure a flexible and professional solution for SKA telescope.

VII. Future Work

The authors consider that there are three key aspects that must be considered to improve the proposed system presented in this paper. The utilization of different SFPs with variable wavelengths causing calibration problems, the evaluation of the timing system considering diverse atmospheric conditions in the SKA infrastructure and the improvement of the jitter of the frequency dissemination by means of the WR technology. Currently, it is not possible to achieve the 1-ps jitter specification, but some promising results allow using WR for this purpose.

Moreover, the solution is flexible enough to be used in other scientific projects such as Cherenkov telescope array [48], IFMIF-DONES [49], [50], or KM3NET [51], [52].

Acknowledgment

The authors would like to thank the CERN BE-CO-HT Unit, the WR community, Seven Solutions, and other institutions, such as JIVE (especially to P. Boven) for their collaboration testing the WR-ZEN board.

References

[1] K. Kalaitzakis, E. Koutroulis, and V. Vlachos, "Development of a data acquisition system for remote monitoring of renewable energy systems," *Measurement*, vol. 34, no. 2, pp. 75–83, 2003.

[2] C. L. Fontana *et al.*, "A distributed data acquisition system for the sensor network of the TAWARA_RTM project," *Phys. Procedia*, vol. 90, pp. 271–278, Nov. 2017. [Online]. Available: https://www.researchgate.net/profile/Cristiano_Fontana/publication/320662008_A_Distributed_Data_Acquisition_System_for_the_Sensor_Network_of_the_TAWARA_RTM_Project/links/59f34bfba6fdcc075ec33d42/A-Distributed-Data-Acquisition-System-for-the-Sensor-Network-of-the-TAWARA-RTM-Project.pdf

[3] M. D. P. Emilio, *Data Acquisition Systems: From Fundamentals to Applied Design*. Springer, 2013. [Online]. Available: https://www.springer.com/gb/book/9781461442134

[4] *GLONASS*. Accessed: Mar. 2018. [Online]. Available: http://www.glonass-ianc.rsa.ru

[5] European GSA. *Galileo System in the European GSA*. Accessed: Mar. 2018. [Online]. Available: https://www.gsa.europa.eu/european-gnss/galileo/galileo-european-global%-satellite-based-navigation-system

[6] J. Yao, I. Skakun, Z. Jiang, and J. Levine, "A detailed comparison of two continuous GPS carrier-phase time transfer techniques," *Metrologia*, vol. 52, no. 5, p. 666, 2015. [Online]. Available: http://stacks.iop.org/0026-1394/52/i=5/a=666

[7] NTP Foundation. *NTP Standard*. Accessed: Mar. 2018. [Online]. Available: http://www.ntp.org

[8] *IEEE Standard for a Precision Clock Synchronization Protocol for Networked Measurement and Control Systems*, IEEE Standard 1588-2002, 2002. Accessed: Mar. 2018. [Online]. Available: https://standards.ieee.org/findstds/standard/1588-2002.html

[9] *Precision Time Protocol Telecom Profile for Phase/Time Synchronization With Full Timing Support From the Network*, document ITU-TG.8275.1/Y.1369.1, 2016. Accessed: Mar. 2018. [Online]. Available: https://www.itu.int/rec/dologin_pub.asp?lang=e&id=T-REC-G.8275.1-201606-I!!PDF-E&type=items

[10] I. Colak, S. Sagiroglu, G. Fulli, M. Yesilbudak, and C.-F. Covrig, "A survey on the critical issues in smart grid technologies," *Renew. Sustain. Energy Rev.*, vol. 54, pp. 396–405, Feb. 2016.

[11] S. Lee, J. Kang, S. S. Choi, and M. T. Lim, "Design of PTP TC/slave over seamless redundancy network for power utility automation," *IEEE Trans. Instrum. Meas.*, vol. 67, no. 7, pp. 1617–1625, Jul. 2018.

[12] M. Agustoni and A. Mortara, "A calibration setup for IEC 61850-9-2 devices," *IEEE Trans. Instrum. Meas.*, vol. 66, no. 6, pp. 1124–1130, Jun. 2017.

[13] *SKA Project*. Accessed: Mar. 2018. [Online]. Available: https://www.skatelescope.org

[14] *SKA Signal and Data Transport Element*. Accessed: Mar. 2018. [Online]. Available: https://www.skatelescope.org/sadt

[15] OHWR. *White Rabbit*. Accessed: Mar. 2018. [Online]. Available: http://www.ohwr.org/projects/white-rabbit/wiki

[16] P. Dewdney. (2015). *Ska1 System Baseline Description V2*. Accessed: Mar. 2018. [Online]. Available: https://www.skatelescope.org/wp-content/uploads/2014/03/SKA-TEL-SKO-000%0308_SKA1_System_Baseline_v2_DescriptionRev01-part-1-signed.pdf

[17] SKA. *MeerKAT Radio Telescope*. Accessed: Mar. 2018. [Online]. Available: http://www.ska.ac.za/gallery/meerkat

[18] CSIRO. *Australia Telescope National Facility*. Accessed: Mar. 2018. [Online]. Available: http://www.atnf.csiro.au/projects/askap/index.html

[19] P. Boven, "Testing WR for SKA in South Africa desert," in *Proc. 9th WR Workshop*, Amsterdam, The Netherlands, 2016. [Online]. Available: https://www.ohwr.org/projects/white-rabbit/wiki/mar2016meeting and https://www.ohwr.org/attachments/4266/5_White_Rabbit_tests_for_the_SKA_in_SA.pdf

[20] Y.-H. Choi, "Theoretical analysis of generalized sagnac effect in the standard synchronization," *Can. J. Phys.*, vol. 95, no. 8, pp. 761–766, 2017.

[21] E. P. Boven, "White Rabbit in radio astronomy," presented at the 16th Int. Conf. Accel. Large Exp. Control Syst. (ICALEPCS), Barcelona, Spain, Oct. 2017, Paper TUCPL03. [Online]. Available: http://accelconf.web.cern.ch/AccelConf/icalepcs2017/talks/tucpl03_talk.pdf

[22] T. Włostowski, "Precise time and frequency transfer in a white Rabbit network," M.S. thesis, Warsaw Univ. Technol., Warszawa, Poland, 2011. [Online]. Available: http://white-rabbit.web.cern.ch/documents/Precise_time_and_frequency_transfer_in_a_White_Rabbit_network.pdf

[23] OHWR. *OHWR Repository*. Accessed: Mar. 2018. [Online]. Available: http://www.ohwr.org

[24] Creotech. *Projects by the Creotech*. Accessed: Mar. 2018. [Online]. Available: http://creotech.pl/en/wr-syntef

[25] *Projects by the Seven Solutions*. Accessed: Mar. 2018. [Online]. Available: http://sevensols.com/index.php/projects

[26] M. Lipinski. (2015). *White Rabbit Robustness & Standardization Work in Progress*. Accessed: Mar. 2018. [Online]. Available: http://mlipinsk.web.cern.ch/mlipinsk/myPage/docs/presentations/WR_Macie%j_TC_2015.pdf

[27] P. Moreira and I. Darwazeh, "Digital femtosecond time difference circuit for CERN's timing systems," in *Proc. London Commun. Symp.*, 2011. [Online]. Available: http://www.ee.ucl.ac.uk/lcs/previous/LCS2011/LCS1136.pdf

[28] G. Daniluk. *White Rabbit Calibration Procedure*. Accessed: Mar. 2018. [Online]. Available: https://www.ohwr.org/documents/213

[29] G. Giorgi and C. Narduzzi, "Precision packet-based frequency transfer based on oversampling," *IEEE Trans. Instrum. Meas.*, vol. 66, no. 7, pp. 1856–1863, Jul. 2017.

[30] G. Giorgi, "An event-based Kalman filter for clock synchronization," *IEEE Trans. Instrum. Meas.*, vol. 64, no. 2, pp. 449–457, Feb. 2015.

[31] N. Kaur, F. Frank, P.-E. Pottie, and P. Tuckey, "Time and frequency transfer over a 500 km cascaded white Rabbit network," in *Proc. EFTF-IFCS*, Jul. 2017, pp. 86–90.

[32] G. Daniluk, "White Rabbit PTP core, the sub-nanosecond time synchronization over Ethernet," M.S. thesis, Warsaw Univ. Technol., Warszawa, Poland, 2012. Accessed: Mar. 2018. [Online]. Available: http://www.ohwr.org/attachments/1368/GD_mgr.pdf

[33] J. L. Gutiérrez-Rivas, C. Prados, and J. Díaz, "Sub-nanosecond synchronization accuracy for time-sensitive applications on industrial networks," in *Proc. EFTF*, Apr. 2016, pp. 1–4.

[34] J. L. Gutiérrez-Rivas, J. López-Jiménez, E. Ros, and J. Díaz, "White Rabbit HSR: A seamless sub-nanosecond redundant timing system with low-latency data capabilities for smart grid," *IEEE Trans. Ind. Informat.*, to be published. [Online]. Available: http://ieeexplore.ieee.org/stamp/stamp.jsp?tp=&arnumber=8125717&isnumber=4389054, doi: 10.1109/TII.2017.2779240.

[35] OHWR. *WRS Repository*. Accessed: Mar. 2018. [Online]. Available: http://www.ohwr.org/projects/white-rabbit/wiki/Switch

[36] *SPEC Board*. Accessed: Mar. 2018. [Online]. Available: http://www.ohwr.org/projects/spec/wiki

[37] Seven Solutions. *Timing Product Page*. Accessed: Mar. 2018. [Online]. Available: http://sevensols.com/index.php/timing-products

[38] M. J. López, J. L. G. Rivas, and J. D. Alonso, "A white-Rabbit network interface card for synchronized sensor networks," in *Proc. IEEE SENSORS*, Nov. 2014, pp. 2000–2003.

[39] ARM. *ARM Processors*. Accessed: May 2018. [Online]. Available: https://www.arm.com/products/processors

[40] F. Torres-González, J. Díaz, E. Marín-López, and R. Rodriguez-Gómez, "Scalability analysis of the white-Rabbit technology for cascade-chain networks," in *Proc. ISPCS*, Sep. 2016, pp. 1–6.

[41] M. Jiménez-López, J. L. Gutiérrez-Rivas, J. Díaz, E. López-Marín, and R. Rodríguez, "WR-ZEN: Ultra-accurate synchronization SoC based on Zynq technology," in *Proc. Eur. Freq. Time Forum (EFTF)*, Apr. 2016, pp. 1–4.

[42] J. Sánchez-Garrido, A. M. López-Antequera, M. Jiménez-López, and J. Díaz, "Sub-nanosecond synchronization over 1G Ethernet data links using white Rabbit technologies on the WR-ZEN board," in *Proc. TSP*, Jul. 2017, pp. 688–693.

[43] J. López-Jiménez, M. Jiménez-López, J. Díaz, and J. L. Gutiérrez-Rivas, "White-Rabbit-enabled data acquisition system," in *Proc. EFTF-IFCS*, Jul. 2017, pp. 410–416.

[44] OHWR. *Fine Delay FMC*. Accessed: Mar. 2018. [Online]. Available: http://www.ohwr.org/projects/fmc-delay-1ns-8cha/wiki

[45] M. Rizzi, "White Rabbit switch performance in grandmaster mode," CERN, Geneva, Switzerland, Tech. Rep., 2016, p. 20. [Online]. Available: https://www.ohwr.org/documents/475 and https://managed-cern-production-bucket-lhoz0gl12lnv.s3-eu-west-1.amazonaws.com/uploads/attachment/file/4467/Report_WRS_MR_rev02.pdf?X-Amz-Expires=600&X-Amz-Date=20180709T195337Z&X-Amz-Algorithm=AWS4-HMAC-SHA256&X-Amz-Credential=AKIAIPK5THR3DIK5DF2Q/20180709/eu-west-1/s3/aws4_request&X-Amz-SignedHeaders=host&X-Amz-Signature=0cb5b8139610f44c4101400c78f75a6b0cc2fbe000ace556a6e9e9b0629a498d

[46] T. Kato, Y. Koyano, and M. Nishimura, "Temperature dependence of chromatic dispersion in various types of optical fiber," *Opt. Lett.*, vol. 25, no. 16, pp. 1156–1158, 2000.

[47] *Joint Institute for VLBI ERIC*. Accessed: Mar. 2018. [Online]. Available: https://www.jive.nl

[48] *Cherenkov Telescope Array*. Accessed: Mar. 2018. [Online]. Available: https://www.cta-observatory.org

[49] *The IFMIF Project*. Accessed: Mar. 2018. [Online]. Available: http://www.ifmif.org

[50] C. de la Morena *et al.*, "Fully digital and white Rabbit synchronized low level RF system for LIPAc," *IEEE Trans. Nucl. Sci.*, vol. 65, no. 1, pp. 514–522, Jan. 2017.

[51] *KM3NeT*. Accessed: Mar. 2018. [Online]. Available: http://www.km3net.org
[52] D. Real *et al.*, "KM3NeT on-shore station and broadcast customization of white-Rabbit switches towards optimizing communication resources for shared control link," in *Proc. TIPP*, 2014. [Online]. Available: http://www.tipp2014.nl/Tipp2014Posters.pdf

Miguel Jiménez-López received the M.Sc. degree in computer science from the University of Granada, Granada, Spain, in 2013, where he is currently pursuing the Ph.D. degree in computer science with the Department of Computer and Technology.

His current research interests include high accurate synchronization protocols specially White Rabbit and the high bandwidth systems using high-speed interfaces such as 10-Gigabit Ethernet.

Felipe Torres-González received the M.Sc. degree in data science and computer engineering from the University of Granada, Granada, Spain, in 2017, where he is currently pursuing the Ph.D. degree in synchronization systems with a focus on high accuracy synchronization systems for scientific deployments.

He is currently a Research Assistant with the University of Granada.

Jose Luis Gutiérrez-Rivas received the M.Sc. degree in computer science from the University of Granada, Spain, in 2009, where he is currently pursuing the Ph.D. degree in computer science with the Department of Computer Architecture and Technology.

He is currently a Software Engineer with Seven Solutions S.L., Granada. His current research interests include safety-critical systems, time and frequency distribution and network dependability, fault tolerance, and reliability.

Manuel Rodríguez-Álvarez received the B.Sc. degree in electronics and the Ph.D. degree in physics from the University of Granada, Granada, Spain, in 1986 and 2002, respectively.

He is currently an Associate Professor with the Department of Computer Architecture and Technology, University of Granada. He collaborates with research facilities as SKA involved in subnanosecond time transfer solutions based on white rabbit. His current research interests include the dissemination of precise timing over optical fiber networks.

Javier Díaz received the M.S. degree in electronics engineering and the Ph.D. degree in electronics from the University of Granada, Granada, Spain, in 2002 and 2006, respectively.

He is currently an Associate Professor with the Department of Computer Architecture and Technology, University of Granada. His current interests include high-performance image processing architectures, safety-critical systems, highly accurate time synchronization, and frequency distribution techniques.